Ecosystems
https://doi.org/10.1007/s10021-022-00787-0

Biophysical Factors Influence Methane Fluxes in Subtropical Freshwater Wetlands Using Eddy Covariance Methods

Zhuoran Yu,[1] Christina L. Staudhammer,[1] Sparkle L. Malone,[2] Steven F. Oberbauer,[2] Junbin Zhao,[3] Julia A. Cherry,[1] and Gregory Starr[1]*

[1]*Biological Sciences Department, The University of Alabama, Tuscaloosa, Alabama 35487, USA;* [2]*Department of Biological Sciences, Florida International University, Miami, Florida 33132, USA;* [3]*Department Biogeochemistry and Soil Quality, Division of Environment and Natural Resources, Norwegian Institute of Bioeconomy Research, Ås, Norway*

Abstract

Wetlands are the largest natural source of methane (CH_4); however, the contribution of subtropical wetlands to global CH_4 budgets is still unclear due to difficulties in accurately quantifying CH_4 emissions from these complex ecosystems. Both direct (water management strategies) and indirect (altered weather patterns associated with climate change) anthropogenic influences are also leading to greater uncertainties in our ability to determine changes in CH_4 emissions from these ecosystems. This study compares CH_4 fluxes from two freshwater marshes with different hydroperiods (short versus long) in the Florida Everglades to examine temporal patterns and biophysical drivers of CH_4 fluxes. Both sites showed similar seasonal patterns across years with higher CH_4 release during wet seasons versus dry seasons. The long hydroperiod site showed stronger seasonal patterns and overall, emitted more CH_4 than the short hydroperiod site; however, no distinctive diurnal patterns were observed. We found that air temperature was a significant positive driver of CH_4 fluxes for both sites regardless of season. In addition, gross ecosystem exchange was a significant negative predictor of CH_4 emissions in the dry season at the long hydroperiod site. CH_4 fluxes were impacted by water level and its changes over site and season, and time scales, which are influenced by rainfall and water management practices. Thus with increasing water distribution associated the Comprehensive Everglades Restoration Plan we expect increases in CH_4 emissions, and when couple with increased with projected higher temperatures in the region, these increases may be enhanced, leading to greater radiative forcing.

Key words: Methane; Eddy covariance; Wetland; Ameriflux; Carbon dynamics; Hydroperiod.

Received 21 December 2021; accepted 12 August 2022

Supplementary Information: The online version contains supplementary material available at https://doi.org/10.1007/s10021-022-00787-0.

Author Contributions: ZY wrote the paper, aided in data curation and analyses, GS, CS, SO conceived the study, performed research, analyzed data, and contributed to writing the paper. SM, JZ collected data, performed and helped with revisions of the paper.

Corresponding author; e-mail: gstarr@ua.edu

Published online: 26 September 2022

Highlights

- Methane flux was measured continuously in subtropical wetlands for 5 years.

- Air temperature and water level were significant drivers of CH_4 fluxes in both sites.
- The long-hydroperiod site had greater CH_4 emission than the short-hydroperiod site.

Introduction

Atmospheric concentrations of methane (CH_4) are now 2.6 times higher than that of preindustrial levels. After a period of stability from 1999 to 2006, concentrations began to increase again in 2007 (Lan and others 2021). Isotopic evidence supports the argument that this increase is associated with biogenic sources (Saunois and others 2020). However, estimates of atmospheric CH_4 concentrations and CH_4 budgets have large uncertainties due to current approaches (Dlugokencky and others 2009; Saunois and others 2020; Lan and others 2021). Moreover, the largest uncertainty in biogenic CH_4 emissions is associated with natural wetlands, which are estimated to contribute about 20–40% of global CH_4 emissions (Ciais and others 2013). Therefore, understanding the drivers of CH_4 emissions from natural wetlands is an essential step in understanding and mitigating global change in the future. Quantifying these emissions is difficult, due to the complexities of wetlands and the fact that climate change is leading to feedbacks that are predicted to increase CH_4 emissions from these ecosystems (Kirschke and others 2013; Bloom and others 2010; Delwiche and others 2021; Zhang and others 2022).

Wetland CH_4 emissions are known to vary due to several biophysical factors. Hydrology, precipitation, temperature and productivity are some of these key factors (Ma and others 2021; Rosentreter and others 2021; Jeffrey and others 2019; Whiting and Chanton 1993; Kim and others 1999; Whalen and Reeburgh 1996). Increasing periods of inundation and water availability have been shown to increase CH_4 emissions in some wetlands (Zhang and others 2022; Were and others 2021; Liu and others 2019; Jeffrey and others 2019). In other ecosystems, temperature plays a role, with increasing temperatures leading to greater emissions rates (Chang and others 2021). And in other cases, water availiblity interacts with temperature, which alters methane emissions (Bansal and others 2016).

Some research has suggested clear seasonal patterns of CH_4 fluxes that are associated with changing weather (Helbig and others 2017; Yu and others 2017). In addition, some studies have suggested surface energy fluxes, vapor pressure deficit (VPD), wind speed and friction velocity (U*) as possible predictors of CH_4 emissions (Alberto and others 2014; Dai and others 2019). The task of untangling uncertainties in predicting and modeling CH_4 is further complicated by the fact that climate change is expected to alter precipitation and temperature patterns across the globe, which will affect wetlands and their carbon dynamics in ways that are not yet understood. Therefore, there is a great need for increasing our temporal and spatial understanding of CH_4 emissions.

The development of Eddy Covariance (EC) methods has enabled greater insight into the drivers and patterns of CH_4 fluxes over large areas and different temporal scales. It also provides more accurate estimation for seasonal and yearly CH_4 budgets (Detto and others 2011; McDermitt and others 2011; Peltola and others 2013, 2014). The EC technique is currently widely used in temperate wetlands but to a lesser extent in tropical systems, although these latter systems are predicted to be a significant contributor to the biogenic emissions of CH_4 (Morin and others 2014; Knox and others 2015; Li and others 2019).

Greater uncertainties can occur in monitoring CH_4 emissions in ecosystems with tropical climate because of the year-round growing season. Also, natural wetland hydrology is more complicated than that of artificial wetlands; artificial wetlands have water management strategies associated with a clear growing season, while in natural wetlands, water table variation occurs during the year with varying weather conditions (Dai and others 2019; Malone and others 2014; Zhao and others 2018), and the natural hydrology patterns can be altered by water management activities. Both challenges are present in our study sites in the Florida Everglades, due to its year-round growing season and complex hydrology driven by natural water flow and rainfall that is coupled with water management practices.

The Everglades is the largest subtropical wetland in the United States, but is subject to tropical climate, with distinctive wet and dry seasons (Beck and others 2005; Kottek and others 2006). Hydroperiods in these freshwater marshes are determined by natural water inputs (precipitation) and outputs (evapotranspiration and drainage) as well as anthropogenic water control from the South Florida Water Management District, all of which affect water levels and inundation periods and ultimately ecosystem carbon dynamics (Davis and Ogden 1994; Burba and others 1999; SFWMD 1999). In recognition of human impacts on Everglades' hydrology, the Comprehensive Everglades

Restoration Plan (CERP) has been implemented with the aim of protecting Everglades ecosystems and restoring historic hydrological patterns (Haman and Svendsen 2006; WRDA 2000). As the CERP restores historic sheet flow in the Everglades (WRDA 2000), CH_4 release is expected to be impacted again by this changing hydrology (Davis and Ogden 1994). However, to date, no studies have continuously measured CH_4 emissions and their drivers in this dynamic system. Thus, this study aimed to investigate CH_4 emissions from Everglades freshwater wetlands, utilizing two sites with different hydrologic regimes (short vs. long hydroperiod). As the first continuous study of CH_4 emissions from this area, our result will improve understanding of the biophysical factors controling CH_4 dynamics, which will allow better estimates of how variability in climate and water management practices will impact CH_4 emission.

With data collected via the EC method from 2016 to 2020, we will address the following questions: (1) what are the seasonal and diurnal patterns of CH_4 fluxes in the two sites? (2) what biophysical factors are significant in predicting CH_4 emissions by site and season? and (3) does the long-hydroperiod site have more CH_4 emissions than the short-hydroperiod site, and are the same biophysical factors driving emission rates at the two sites?

Materials and Methods

Study Site Description

The study was conducted in Everglades National Park at Taylor Slough (TS/Ph-1; 25°26′16.5″N, 80°35′40.68″W) and Shark River Slough (SRS-2; 25°33′6.72″N, 80°46′57.36″W). These sites are part of the Florida Coastal Everglades Long Term Ecological Research project (FCE-LTER) and are AmeriFlux sites. The region is classified as subtropical with tropical climate and has mean annual rainfall of 1430 mm with distinct wet and dry seasons (Duever and others 1994; National Climatic Data Center, NCDC, http://www.ncdc. noaa.gov/). The wet season occurs from May to November, with temperatures from 30 to 35 °C. The dry season extends from December to mid-May when temperatures range from 12 to 24 °C. Approximately 60% of rain occurs during the wet season, with interannual variability in rainfall patterns (Duever and others 1994; Obeysekera and others 1999).

TS/Ph-1 is characterized by a thin layer (~ 0.14 m) of marl overlying limestone bedrock while SRS-2 has a layer (~ 1 m) of peat soils overlying limestone bedrock with extensive slough and ridge microtopography (Duever and others 1976). Sawgrass (*Cladium jamaicense* Crantz) is the dominant species in both sites. At TS/Ph-1, muhly grass (*Muhlenbergia filipes* M.A. Curtis) is co-dominant with sawgrass. Ridges at SRS-2 are predominantly sawgrass while sloughs contain *Eleocharis sp.* and *Panicum sp.* interspersed with water lilies, *Nymphaea odorata* Aiton (Armentano and others 2006; Gottlieb and others 2006). The mean canopy height for TS/Ph-1 is ~ 0.73 m, whereas the mean canopy height for SRS-2 is about 1.02 m (Malone and others 2014). Although these two sites are only about 23 km apart, there is a noticeable hydroperiod length difference. TS/Ph-1 is inundated for 4 to 6 months each year during the wet season, whereas SRS-2 is inundated ~ 12 months a year. However, water levels in SRS-2 can drop below the peat surface during extreme dry seasons with uncharacteristically low precipitation (Davis and Ogden 1994; Malone and others 2014).

Field Measurements

Eddy Covariance Method

Open-path infrared gas analyzers were used to measure CH_4 (mol m^{-3}; IRGA, LI-7700, Li-COR Inc., Lincoln, NE), CO_2 (mg mol^{-1}; IRGA, LI-7500, Li-COR Inc., Lincoln, NE) and water vapor (ρ_v; mg mol^{-1}), and a paired sonic anemometer (CSAT3, Campbell Scientific Inc., Logan, UT) measured sonic temperature (T_s; K) and 3-dimensional wind speed (u, v and w, respectively; m s^{-1}). These paired sensors were 0.09 m apart and installed at 3.30 and 3.24 m above ground level (a.g.l.) at TS/Ph-1 and SRS-2, respectively. The EC data were collected on the LI-COR Biomet data acquisition system on the LI-7550 analyzer interface unit (LI-COR Inc., Lincoln, NE) and stored on an industrial 16 GB USB drive. Both LI-7500 IRGAs were calibrated monthly using a trace gas standard for CO_2 in air (+ 1.0%), dry N_2 gas and a portable dewpoint generator (LI-610, LI-COR Inc.). The data gaps at both sites from September through October 2017 were the result of damage to the towers and closure of Everglades National Park after Hurricane Irma made landfall on 9 September 2017. Footprint analyses (Kljun and others 2002, 2004) indicated that 80% of measured fluxes were within 100 m radius of both flux towers. The vegetation in the footprint at TS/Ph-1 is relatively uniform for 500 m in all directions whereas at SRS-2 the vegetation in the predominant wind direction (easterly) is a mix of slough and ridge.

CH_4 Flux Calculation

Fluxes based on mass density (ρ_{CH4}) measurements by the LI-7700 were calculated according to McDermitt and others (2011; Eq. 1):

$$F_{CH_4} = A\left(\overline{w'\rho'_{CH_4}}\right) + B\mu\frac{\overline{\rho_{CH_4}}}{\overline{\rho_a}}\overline{w'\rho'_{H_2O}} + C\frac{(1+\mu\sigma)\overline{\rho_{CH_4}}}{\overline{T}}\overline{w'Ta'} \quad (1)$$

where *A*, *B*, and *C* are dimensionless multipliers to correct for spectroscopic effects caused by temperature- and pressure-induced line-broadening, μ is the molar mass ratio of dry air to water vapor, ρ_a is the average mass density of dry air, σ is the mass density ratio of water vapor to dry air, ρ_{H2O} is the water vapor mass density, and *Ta* is air temperature (°C). Data are presented following the atmospheric convention that fluxes to the atmosphere are positive and from the atmosphere are negative.

Meteorological Variables

At each site, meteorological variables were measured at 15-s and collected as half-hourly averages on a data logger (CR1000, Campbell Scientific Inc), including: Ta (°C) and relative humidity (Rh; %) (HMP45C, Vaisala, Helsinki, Finland) mounted within an aspirated shield (43,502, R.M. Young Co., Traverse City, MI), and barometric pressure (P; Pa) (PTB110, Vaisala). The Ta/Rh sensors were installed at the same height a.g.l. as the IRGA and CSAT.

Other meteorological data were measured every 15-s and collected as 30-min averages through a multiplexer (AM16/32A Campbell Scientific Inc.) with another datalogger (CR10X Campbell Scientific Inc.). This included photosynthetically active radiation (PAR; µmol m^{-2} s^{-1}) (PAR Lite, Kipp and Zonen Inc., Delft, the Netherlands), incident solar radiation (R_s; W m^{-2}) (LI-200SZ, LI-COR Inc.), and net radiation (R_n; W m^{-2}) (CNR2-L, Kipp and Zonen). Precipitation measurements were made with tipping bucket rain gages (mm) (TE525, Texas Electronics Inc., Dallas, TX). Soil volumetric water content (VWC; %) was calculated from equations developed for peat and marl soils using the methodology of Veldkamp and O'Brien (2000), from the dielectric constant using two soil moisture sensors (CS616, Campbell Scientific Inc.) installed at a 45° angle at the soil surface at each site. Soil temperature (T_s; °C) was measured at 5 cm, 10 cm, and 20 cm depths at two locations within each site using insulated thermocouples (Type-T, Omega Engineering Inc., Stamford, CT). When inundated at SRS-2, water temperature (T_w; °C) was measured using two pairs of insulated thermocouples (Type-T, Omega Engineering Inc.), each pair located at a fixed height 5 cm above the soil surface, and another attached to shielded floats that held the thermocouples 5 cm below the water surface. At TS/Ph-1, T_w was measured using insulated thermocouples (Type-T, Omega Engineering Inc.) located at a fixed height 2 cm below the water surface. Water level (m) at both sites was recorded every half-hour with a water level logger (HOBO U20-001–01, Onset Computer Corporation, Bourne, MA).

Data Processing and Quality Control

Raw CH_4 EC data were processed with EddyPro Software (Advanced mode, version 6.2.1, LI-COR Inc., Lincoln, NE, USA) over 30 min time intervals. The raw CH_4 turbulence data were processed with the LI-7700 diagnostics turned off. Using the Advanced mode, the following were chosen as processing options: double rotation for tilt correction, block averaging for turbulent fluctuations, covariance maximization with default for time lags compensation, and compensate density fluctuations (WPL terms). Spectral analyses and corrections were performed following Moncrieff and others (2005). The half-hourly data were filtered when signal strength was low (RSSI < 10%), during rainfall events, and when outside of a biologically reasonable range of − 0.25 to 2 (µmol m^{-2} s^{-1}), which allowed for about 90% collected CH_4 half-hourly data to be included in subsequent analyses. U* and quality flags, which are common filters in previous research for CH_4 fluxes, were not considered in this research since no obvious patterns were observed with respect to U* threshold or quality flag number. After filtering, 67.9% (day: 71.5%; night: 64.4%) and 69.5% (day: 74.5%; night: 65.4%) of CH_4 data remained in TS/Ph-1 and SRS-2, respectively.

Raw flux data were processed with EddyPro software (Advanced mode, version 6.2.1, LI-COR Inc., Lincoln, NE, USA) with corrections for density fluctuations and high-frequency spectral loss (Fratini and Mauder 2014). Flux measurements for CO_2 were filtered when systematic errors were indicated, such as: (1) evidence of rainfall, condensation, or bird fouling in the sampling path of the IRGA or sonic anemometer, (2) incomplete half-hour datasets during system calibration or maintenance, (3) poor coupling of the canopy with the external atmospheric conditions, as defined by the friction velocity, U*, using a threshold of 0.15 m s^{-1} (Goulden and others 1996; Clark and others 1999), and (4) excessive variation from the half-hourly mean based on an analysis of standard deviations for u, v, and w wind and CO_2 statistics. Quality assurance of the flux data was also maintained by examining plausibility tests for net ecosystem exchange of CO_2 (NEE) values (that is, $|NEE| < 30$ µmol m^{-2} s^{-1}), stationarity criteria, and integral turbulent statistics (Foken and Wichura 1996; Foken and Leclerc 2004). At TS/Ph-1, 38% and 77% of the day and nighttime NEE data were removed, respectively. At SRS-2, 34% of daytime data and 70% of nighttime NEE data were removed. Missing half-hourly NEE data were gap-filled using separate functions for day and night. When PAR was > 10 W m^{-2}, NEE data were gap-filled using a Michaelis-Menton approach (NEE_{day}; Eq. 2), and when PAR was ≤ 10 W m^{-2}, NEE data were gap-filled using an Arrhenius approach (NEE_{night}; Eq. 3):

$$NEE_{day} = R_{eco} - \frac{\alpha\phi P_{max}}{\alpha\phi + P_{max}} \tag{2}$$

where α is the apparent quantum efficiency, Φ is PAR, R_{eco} is ecosystem respiration (µmol CO_2 m^{-2} s^{-1}), and P_{max} is the maximum ecosystem CO_2 uptake rate (µmol CO_2 m^{-2} s^{-1}).

$$NEE_{night} = R_{eco} = R_0 \exp^{(bTa)} \tag{3}$$

where R_0 is the base respiration rate when air temperature is 0 °C and b is an empirical coefficient. In Eq. 2, R_{eco} is an estimated model parameter, whereas R_{eco} measurements are the dependent variable in Eq. 4. Following gap filling, gross ecosystem exchange of CO2 (GEE) was calculated from half hourly NEE and R_{eco} data (Eq. 4).

$$GEE = NEE - R_{eco} \tag{4}$$

Statistical Analysis

For analyses, we utilized the average CH_4 flux (umol m^{-2} s^{-1}), computed on a daily basis during the study period. To mitigate the possibility of bias due to disproportionate missing nighttime measurements, we only used days that had a minimum of 32 half-hourly CH_4 records after filtering. To investigate the relationship between CH_4 and micrometeorological variables, we calculated daily values of potential drivers such as mean or daily change, using their values only when CH_4 data were present. For each year, we had between 204 and 293 daily values available for analysis (Table 1). The wet season for each year was determined following Noska and Misra (2016) and Misra and others (2018), which estimate the location of inflection points signaling the onset and demise of the cumulative daily anomaly of rainfall (Eq. 5):

Table 1. Number of Days Available for Modeling Daily Methane Fluxes From 2016 to 2020 in TS/Ph-1 and SRS-2

Year	TS/Ph-1	SRS-2
2016*	204	225
2017	275	208
2018	293	289
2019	218	275
2020*	206	224

Leap year with 366 days available

$$P_n'(k) = \sum_{m=1}^{k} \left[P_n(m) - \overline{\overline{P}} \right] \tag{5}$$

where: $P_n(m)$ is the average daily rainfall for day m = 1, …, k of year n over each study site. $\overline{\overline{P}}$ is the overall mean daily rainfall over the entire study period. Because of data gaps in rainfall records for TS/Ph-1, both sites used $\overline{\overline{P}}$ calculated using rainfall from SRS-2 only; however, the onset and demise were determined individually for each site and each year.

To test hypotheses about the drivers of CH_4 fluxes, we estimated generalized additive models (GAMs; Hastie and Tibrishani 1986) for each site. GAMs are a form of Generalized Linear Model where the response variable depends linearly on predictor variables via unknown smooth functions (Wood 2017). This allows for nonlinear behavior while maintaining explainability. We estimated two types of GAMs to determine the potential nonlinear drivers of CH_4 fluxes. The first models included a group of biophysical drivers, whereas the second utilized a set of variables describing the water table dynamics. As an initial step in determining the best set of predictors in GAMs, we performed Pearson correlation analyses for average daily CH_4 and all potential biotic and abiotic drivers. We examined the correlations between daily CH_4 fluxes and twelve drivers suggested by previous research. The groups of variables from each type of GAM could not be combined into an 'overall model' due to their high multicollinearity.

Four biophysical drivers were chosen for the first GAMs based on their high correlations with mean daily CH_4 fluxes and lack of correlation with other selected drivers, which could indicate multicollinearity: average daily air temperature (Ta), average daily water level, average daily gross ecosystem exchange (GEE), and daily atmospheric pressure change (maximum daily pressure minus minimum daily pressure) or daily change in maximum atmospheric pressure (maximum daily pressure on the current day minus that of the previous day). We also included a fixed effect for season (wet versus dry), as well as the interaction of each quantitative predictor variable with season. We used a quasi-backwards stepwise procedure to determine the ''best'' model for each site, dropping the effect with the highest p-value sequentially, and ensuring that each step resulted in a model with a lower (better) AIC (Akaike Information Criterion) value. Either daily pressure change or daily change in maximum pressure was selected based on which had the best (lowest) p-value in the model.

For the second GAMs formulated to explore water level dynamics, we used a 30-day moving average of daily water level, daily water level change (mean daily water level minus that of the previous day), and water level change over 10 days (mean daily water level minus that of the 10 days prior). The moving average of daily water level over 30 days smooths the trend in water level and quantifies prospective as well as longer-term water level conditions, which signal weather events and water management distribution, and could be more extreme under predicted future climate change. The daily water level change represents small time scale water fluctuations, whereas water level change over 10 days explores the direction of water level change over an intermediate time scale.

All four models used data at each site from 2016 to 2020 but excluded the 2016 TS/Ph-1 wet season due to insufficient CH_4 data due to instrumental malfunctions. Using the gam function in the *mgcv* package (Wood 2011), a smoothing spline function via restricted maximum likelihood (REML) was fit to each driver individually. Predicted estimated marginal means from each GAM were calculated to visualize relationships between each significant independent variable and predicted CH_4 using the ''get_gam_predictions'' function (*mgcv* package; Wood 2011). All statistical analyses were performed in R (version 4.0.1) and RStudio (version 1.3.959). We considered differences significant at $p < 0.05$.

Results

Environmental Conditions and Variation

Rainfall patterns and wet season lengths in both sites were similar overall and did not show significant interannual differences in the onset and length of seasons, except in 2019, which had a significantly shorter wet season (Figure S1, Table S1; Supplemental Information). The longest wet season was observed in 2020, lasting from early May to mid-November. Frequent rainfall events occurred during the wet season, and some sporadic rainfall was observed during the dry season.

Compared to other years, 2016 had the fewest days with low water levels during the dry season in both TS/Ph-1 and SRS-2; water levels at TS/Ph-1 remained well above the soil surface the entire dry season. However, the 2016 wet season water levels were the lowest across the whole study period in both sites compared to other years (Figure 1b). The years 2017–20 presented similar patterns with substantial water level differences between wet and dry seasons, especially in the short hydroperiod site. At the end of 2020, due to water management activities, water levels in both sites were higher than normal. As expected, SRS-2 had a higher water level than TS/Ph-1 overall and remained inundated throughout the entire study period (Figure 1b).

Average daily Ta ranges were similar by year at both sites, about 10 to 34 °C during the study period (Figure 1a). The lowest daily temperatures were 9.9 °C and 10.5 °C, and the highest daily temperatures were 32.8 °C and 34.0 °C for TS/Ph-1 and SRS-2, respectively. Unlike the other factors, daily maximum pressure showed a ''W'' shaped pattern within each study year, with higher pressure observed during winter and summer. However, summertime peaks in maximum daily pressure were lower than those of winter in both sites (Figure 1c). The mean pressure for both sites was ~ 1017 Pa, and patterns were very similar across the two study sites.

Time Series of Daily Gross Ecosystem Exchange (GEE)

GEE showed clear seasonal patterns in each study year, with more gross CO_2 uptake during the wet seasons and less gross CO_2 uptake during the dry seasons for both TS/Ph-1 and SRS-2. GEE was highest in 2016 in both sites, which indicated that both sites had less gross CO_2 uptake through photosynthesis in 2016 by the atmospheric convention. The two sites had similar average GEE values over the five years (-1.4 to -1.5 μmol m^{-2} s^{-1}; Figure 1d).

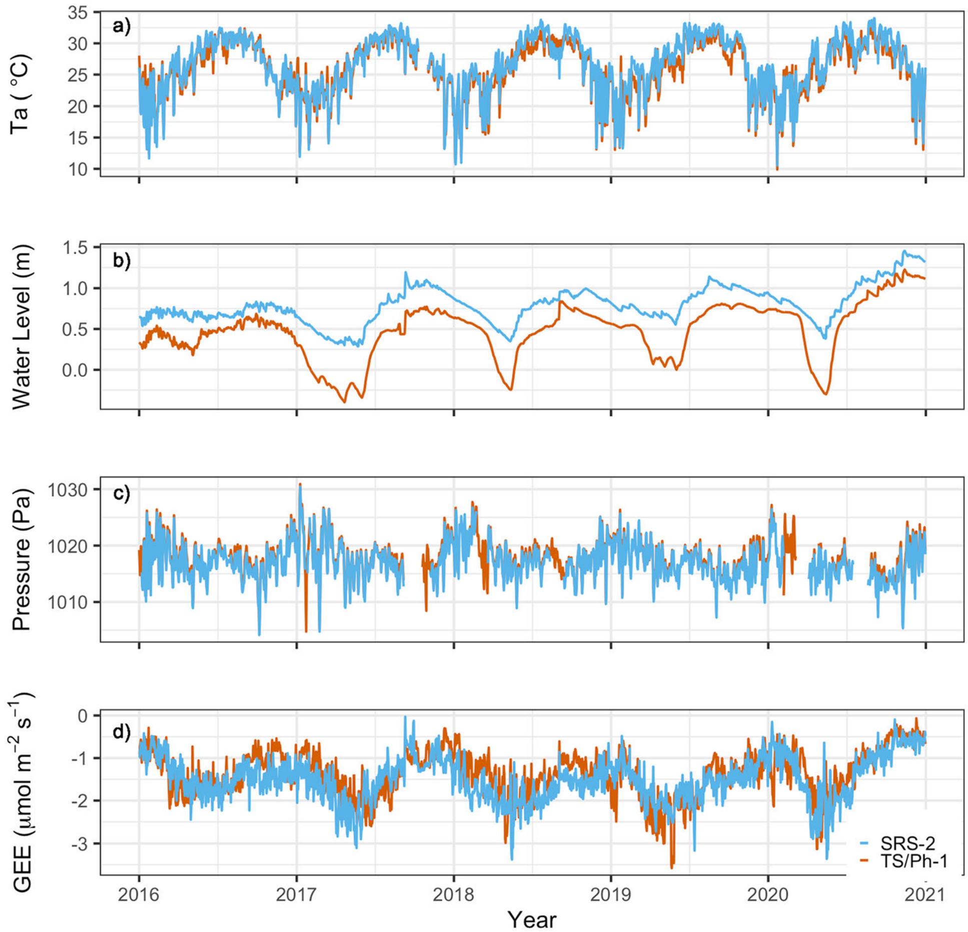

Figure 1. Average daily **a** air temperature (Ta; °C), **b** water level (m), **c** pressure (Pa), and **d** daily gross ecosystem exchange (GEE; μmol m^{-2} $s.^{-1}$) in TS/Ph-1 and SRS-2.

Time Series of Half-Hourly and Daily CH_4 Fluxes

Both sites showed similar seasonal patterns across years, with more CH_4 being released during wet seasons compared to dry seasons (Figure 2). These patterns, however, did not overlap precisely with any potential drivers (Figure 1). Compared to TS/Ph-1, SRS-2 had stronger annual patterns, with greater differences between wet and dry season CH_4 fluxes, except during 2020. Gaps during late 2017 were caused by Hurricane Irma (September 17, 2017) and other gaps occurred due to instrument malfunctions. Several CH_4 emission spikes occurred late 2017 as well as early and mid-2018 in TS/Ph-1 (Figure 2b, c). High values were observed in SRS-2 during late 2016, late 2018 and mid 2019 (Figure 2f, h, i). Both sites had positive mean CH_4 fluxes during the study period, with average CH_4 emissions of 0.034 and 0.081 μmol m^{-2} s^{-1} for TS/Ph-1 and SRS-2, respectively. In addition, SRS-2 also released more CH_4 than TS/Ph-1 during each of the five years (Table 2).

Diurnal patterns in CH_4 fluxes were not as distinctive as seasonal patterns in either site (Figure S2; Supplemental Information). In TS/Ph-1, relatively obvious peaks were observed in late morning in 2017, early afternoon in 2019 and midnight in 2020 (Figure S2b, d). In SRS-2, peaks in CH_4 fluxes in early morning in 2016, and just after midnight in 2018 were relatively higher than other time periods during the day (Figure S2f, h). In addition, mean dry and wet season CH_4 release did not show great diurnal differences, except in 2016 and 2018 in SRS-2, when the wet season emissions were generally higher than that of the dry season, especially in early morning and late evening (Figure S2f, h; Table 2).

Biophysical Model of CH_4

In both TS/Ph-1 and SRS-2, Ta and water level were significant predictors of CH_4 fluxes in both

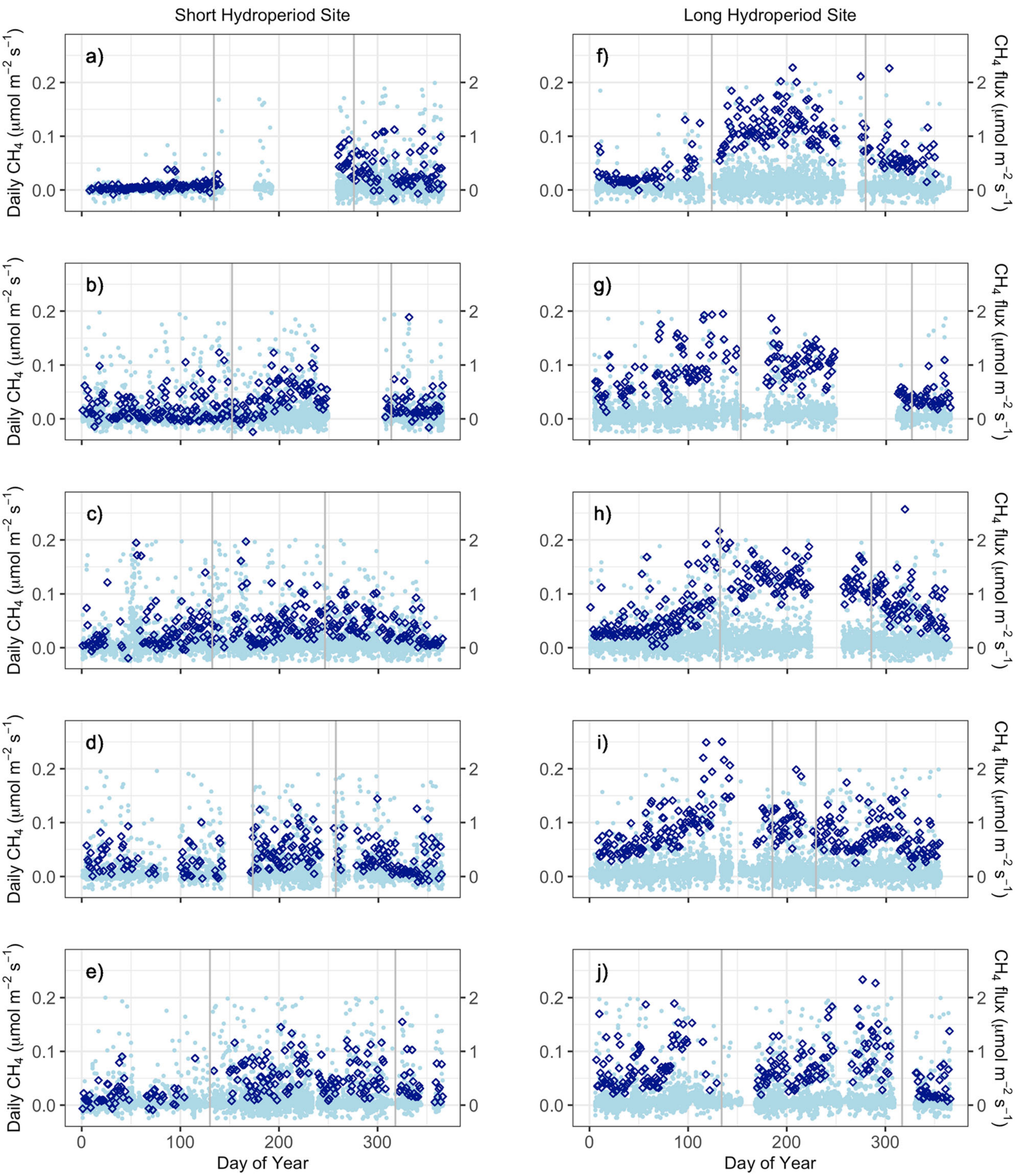

Figure 2. Time series of daily mean CH_4 fluxes (dark blue; refer to left y-axis) and half-hourly CH_4 fluxes (light blue; refer to right y-axis) from 2016 to 2020 in TS/Ph-1 (**a–e**) and SRS-2 (**f–j**).

seasons (Table 3). GEE was also a significant predictor of CH_4 emissions in SRS-2, but only in the dry season. Moreover, neither daily pressure change nor daily change in maximum pressure were significant drivers of CH_4 in either site; therefore, pressure change was dropped from the models to achieve a better (lower) AIC. The model for SRS-2 explained 43.6% of deviance in CH_4,

Table 2. Summary Statistics Describing Daily Average CH_4 Fluxes (μmol m^{-2} s^{-1}) in TS/Ph-1 and SRS-2 From 2016 to 2020

Year	TS/Ph− 1					SRS− 2				
	Min	Max	Average			Min	Max	Average		
			Year	Dry	Wet			Year	Dry	Wet
2016	− 0.034	0.112	0.020	0.020	/	− 0.001	0.227	0.081	0.048	0.120
2017	− 0.034	0.290	0.029	0.024	0.041	0.013	0.195	0.080	0.073	0.100
2018	− 0.020	0.197	0.038	0.041	0.051	0.003	0.320	0.088	0.073	0.137
2019	− 0.010	0.144	0.037	0.034	0.054	0.018	0.311	0.085	0.085	0.093
2020	− 0.034	0.155	0.042	0.029	0.062	0.007	0.233	0.070	0.067	0.084

Table 3. Effective Degrees of Freedom (EDF), Reference Degrees of Freedom (RDF), F Values and Associated p-values for GAMs of Biophysical and Water Dynamics Models by Site

Model	Effect	TS/Ph-1				SRS-2			
		EDF	RDF	*F* value	*p* value	EDF	RDF	*F* value	*p* value
Biophysical	Ta × dry	2.32	2.93	15.24	< 0.001	7.98	8.71	8.06	< 0.001
	Ta × wet	2.67	3.20	14.41	< 0.001	6.95	7.94	12.57	< 0.001
	Water level × dry	5.81	6.84	5.54	< 0.001	3.53	4.43	30.87	< 0.001
	Water level × wet	2.64	3.29	10.02	< 0.001	2.27	2.74	36.02	< 0.001
	GEE × dry					1.00	1.01	23.01	< 0.001
	GEE × wet					1.79	2.30	0.57	0.614
Water dynamics	30-d ma × dry	4.21	5.10	7.86	< 0.001	8.20	8.69	19.08	< 0.001
	30-d ma × wet	1.00	1.01	42.75	< 0.001	8.83	8.98	18.64	< 0.001
	Daily change × dry	2.17	2.81	1.24	0.319	5.09	6.26	5.81	< 0.001
	Daily change × wet	4.88	5.84	4.03	< 0.001	2.81	3.54	2.05	0.080
	10-d change × dry	3.00	3.79	1.98	0.100	3.83	4.79	2.08	0.070
	10-d change × wet	3.70	4.55	2.70	0.026	2.33	2.94	8.01	< 0.001

Ta = daily average temperature (°C), water level (m) is a daily average, GEE = gross ecosystem exchange (μmol m^{-2} s^{-1}; only significant in SRS-2), 30-d ma = moving average water level (m) over 30 days, daily change and 10-d change refer to maximum–minimum water level (m) over the period.

whereas the TS/Ph-1 model had much less explanatory power (deviance explained = 19.4%).

In both TS/Ph-1 and SRS-2, Ta was a strong driver for CH_4 emissions (Figure 3a, c). In the dry season of both sites and the wet season of SRS-2, higher Ta led to greater CH_4 release. During the wet season of TS/Ph-1, more CH_4 was released when Ta was between 20 and 25 °C, and leveled off above 25 °C (Figure 3a). Since both sites lie in a subtropical zone, it is rare to have low temperatures during the summer wet season, and thus, wide confidence intervals were observed in the wet season when Ta was under 20 °C at both sites (Figure 3a, c), reflecting the rarity of these events.

Water level was a significant driver of CH_4 for both sites, but it impacted CH_4 differently by site. Water level generally showed a positive relationship with CH_4 emissions at TS/Ph-1 in both seasons, and the relationship between daily water level and CH_4 fluxes showed greater variance in the dry season than in the wet season. During the dry season, higher water level led to more CH_4 release when water level was very low (< − 0.25 m) and relatively high (> 0.75 m); when water level was between 0 and 0.3 m, there was a drop of CH_4 emission with increased Ta, but CH_4 release increased steeply as water level rose from 0.3 to 0.5 m and then was flat when water level was 0.5–0.75 m (Figure 3b). During the wet season, higher water level led to more CH_4 emissions, and the increase became less steep when water level was higher than 0.5 m (Figure 3b). Water level in SRS-2 also showed a more complex association with CH_4 in the dry season versus the wet season. During the dry season, water level was significantly associated with CH_4, but its effects fluctuated on a small scale as water level rose. In contrast to TS/Ph-1, during the wet season, higher water level led to lower CH_4 release in SRS-2, especially when water level was above 1.25 m (Figure 3d).

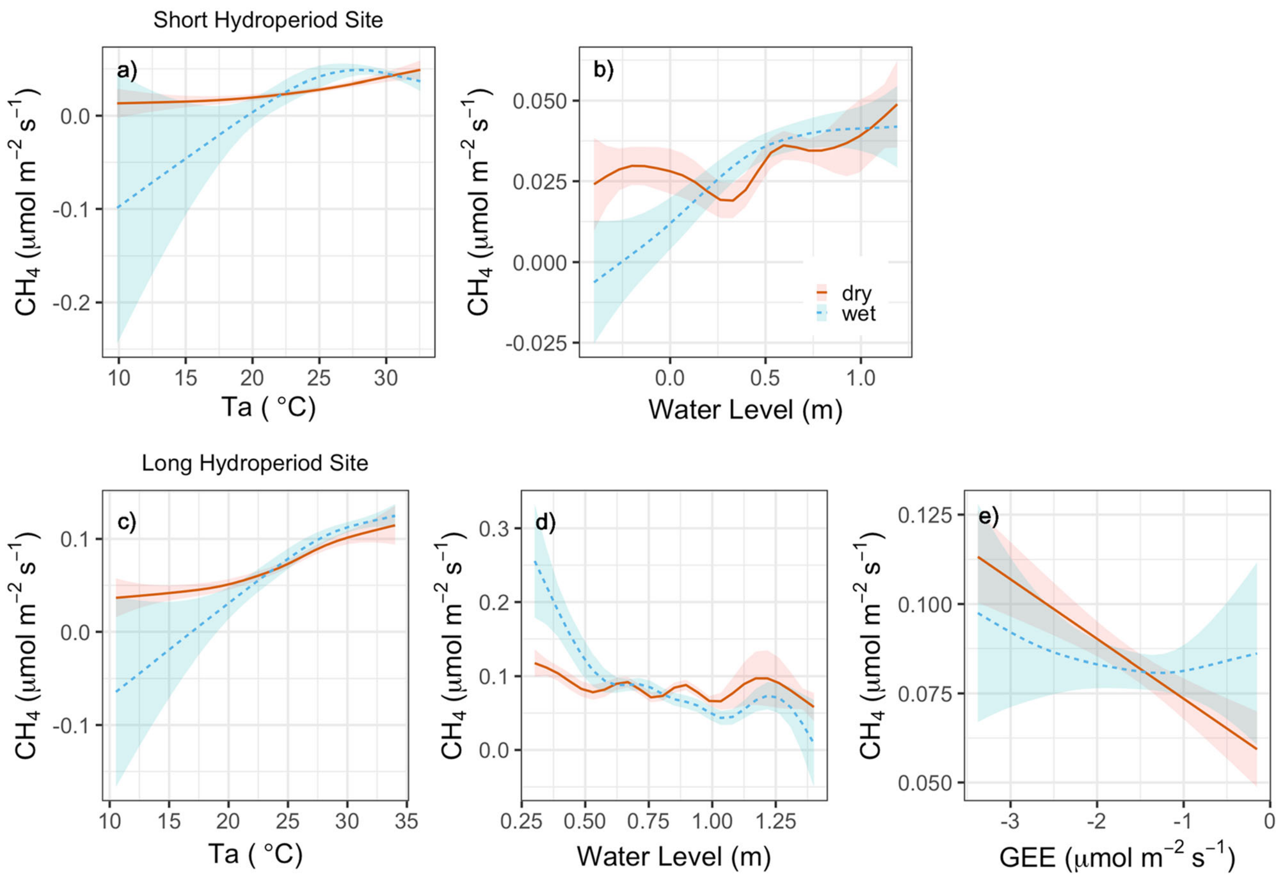

Figure 3. Predicted estimated marginal means from GAM models of CH_4 drivers in TS/Ph-1 **a**, **b** and SRS-2 **c–e**, by: average daily: **a** and **c** air temperature (Ta (°C); dry: $p < 0.001$, wet: $p < 0.001$), **b** and **d** water level (m; dry: $p < 0.001$, wet: $p < 0.001$), and **e** gross ecosystem exchange (GEE (µmol m^{-2} s.$^{-1}$); dry: $p < 0.001$, wet: $p = 0.61$; only significant in SRS-2).

Lastly, GEE did not show a significant relationship with CH_4 fluxes in either season in TS/Ph-1, and therefore was dropped in the model. GEE was associated with CH_4 in SRS-2, but only during the dry season; CH_4 release decreased as GEE increased, that is, when plants were less productive.

Water Level Dynamics Model of CH_4 Fluxes

Although TS/Ph-1 and SRS-2 have different water table depths, variables describing the fluctuations of water level in both sites were similar in their temporal patterns. As with average daily water level, SRS-2 had higher 30-day average water table values versus that of TS/Ph-1 (Figures 1b, 4a, d). While the daily water table changes were similar by site (Figure 4b, e), the intermediate water level change over 10 days showed a clearer seasonal pattern in TS/Ph-1 (Figure 4c, f).

As with the biophysical model, the water dynamics model for SRS-2 had better fit (deviance explained = 0.310) versus that of TS/Ph-1 (deviance explained = 0.169); however, this model explained less variation in CH_4. The 30-day moving average of daily water level was a significant predictor for CH_4 emissions across both seasons in TS/Ph-1 and SRS-2, but it presented different associations across the two sites (Table 3). The impacts of daily and 10-day change in water level, however, depended on season and site. The effect of 30-day moving average on CH_4 fluxes in TS/Ph-1 was similar to that of daily water level in the biophysical model (Figures 3b, 5a). In the dry season, CH_4 emission was negatively associated with water level when it was less than 0.3 m and was positively associated with water level as water level increased above 0.3 m. For wet seasons, greater CH_4 emissions were observed as water level increased (Figure 5a). In SRS-2, the 30-day average water level impacted CH_4 emissions significantly in both seasons, but the wet season association was significantly different from that of daily water level in the

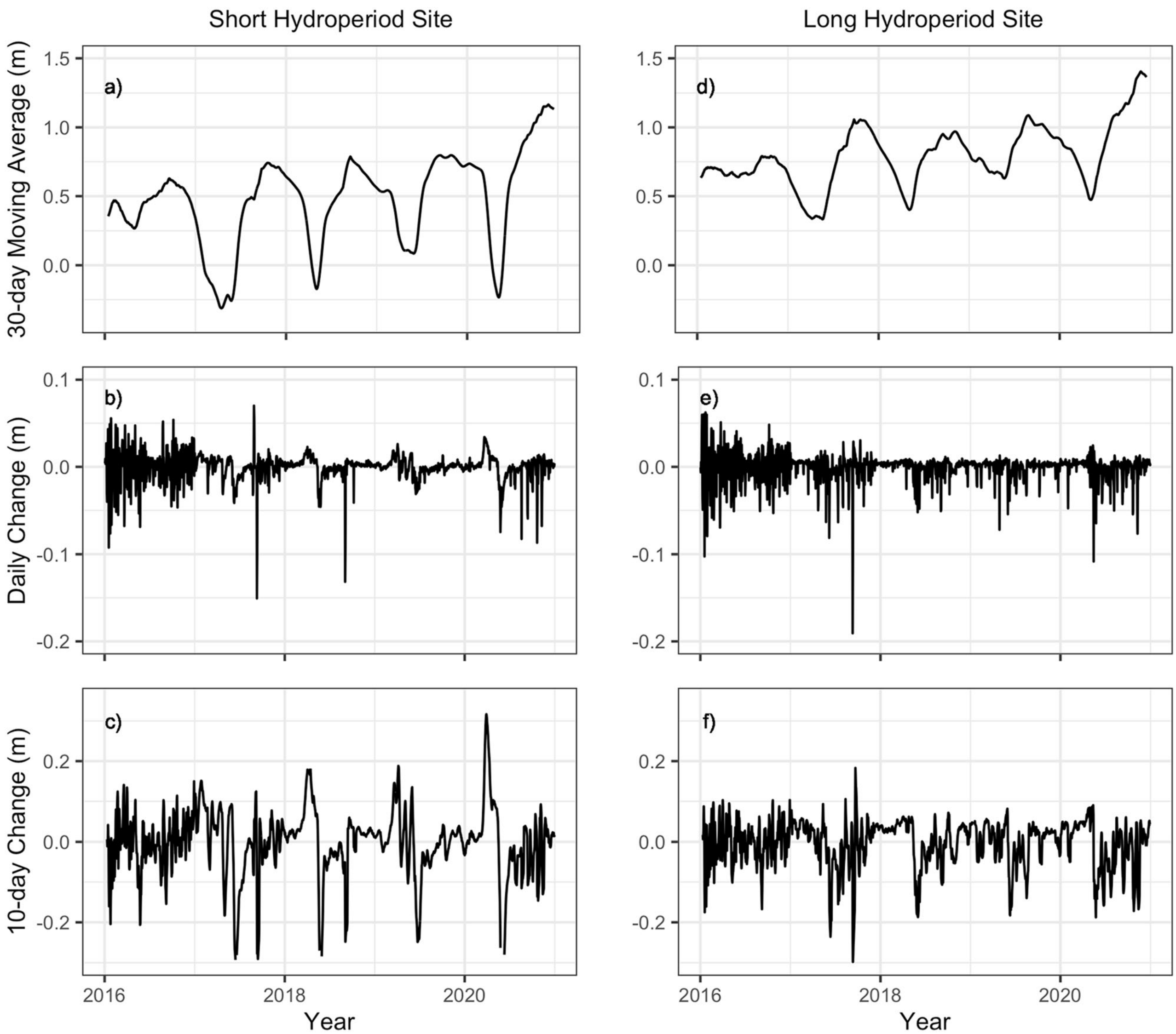

Figure 4. Water dynamics variables in TS/Ph-1 **a–c** and SRS-2 **d–f**: **a** and **d** 30-daily water level moving average (m), **b** and **e** daily water level change (m), and **c** and **f** water level change over 10 days (m).

biophysical model (Figures 3d, 5d). In the dry season, water level increase did not impact CH_4 fluxes except when water level was relatively high ($> \sim 1$ m); higher water level led to more CH_4 release when water level was 1–1.2 m, and led to lower CH_4 release when water level was above 1.2 m. However, a large confidence interval was associated with high water level in the dry season, since high water levels are not common (Figure 5d). The wet season 30-day average water level impact on CH_4 was different from that of the daily mean (Figures 3d, 5d). Higher dry season 30-day water level (> 0.45 m) led to decreased CH_4 emission, but this effect was dampened when water level was above 0.6 m. Very low wet season water level in SRS-2 resulted in the site being a CH_4 sink.

Daily water level change had a strong impact on CH_4 emissions during the wet season in TS/Ph-1 and the dry season in SRS-2 (Figure 5b, e). In TS/Ph-1 during the wet season, a daily increase of 0.025 m or less led to lower CH_4 release, whereas a daily decrease of 0.025 m or less did not have an impact on CH_4 fluxes. In addition, more CH_4 was released in TS/Ph-1 when water level increased more than 0.025 m over the previous day, and less CH_4 emissions occurred when there was a drop in water level greater than 0.025 m (Figure 5b). Daily water level change had a significant impact on CH_4 release in the dry season in SRS-2 (Figure 5e);

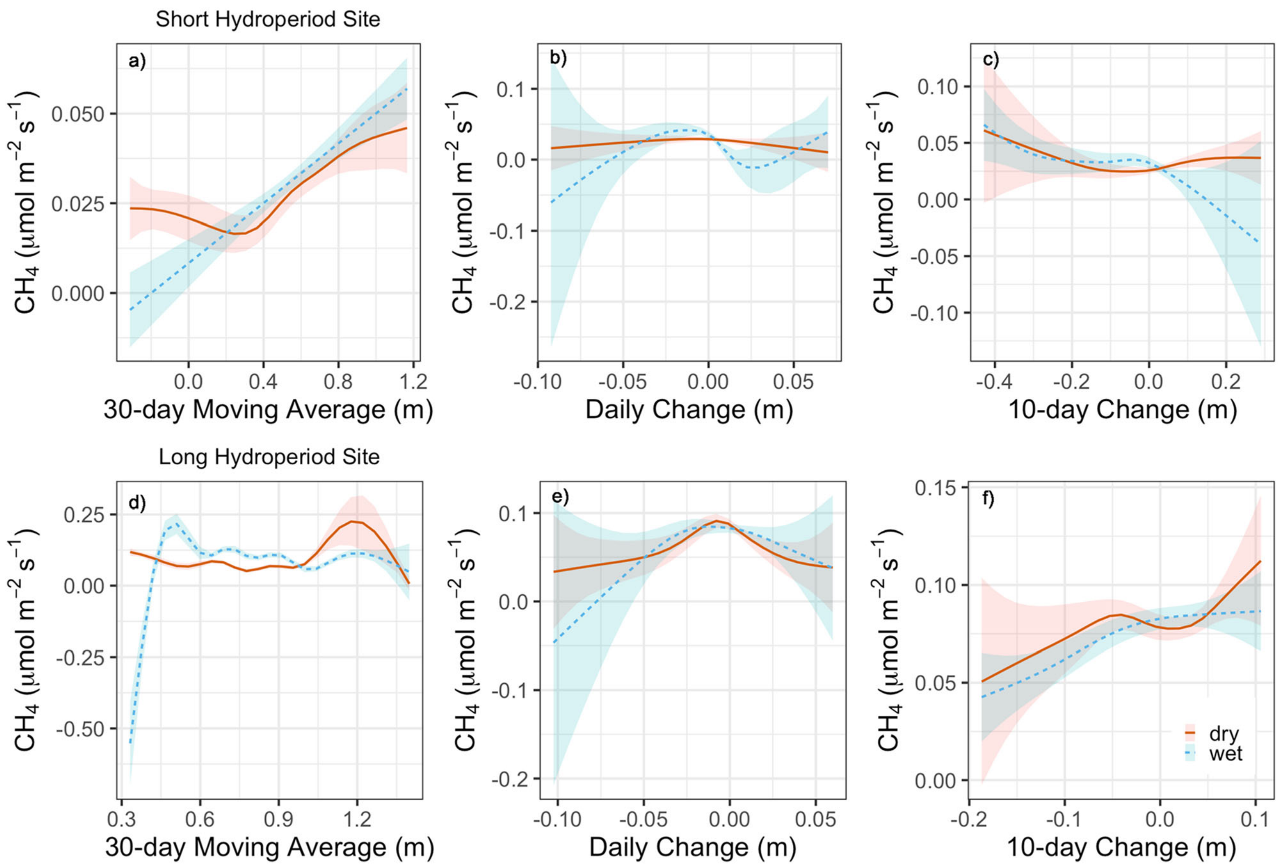

Figure 5. Predicted estimated marginal means from GAM models of CH_4 drivers in TS/Ph-1 **a–c** and SRS-2 **d–f**, by: **a** and **d** 30-daily water level moving average (m; dry: $p < 0.001$, wet: $p < 0.001$), **b** and **e** daily water level change (m; TS/Ph-1 dry: $p = 0.319$, wet: $p < 0.001$; SRS-2 dry $p < 0.001$, wet: $p = 0.08$), **c** and **f** water level change over 10 days (m; TS/Ph-1 dry: $p = 0.100$, wet: $p = 0.026$; SRS-2 dry: $p = 0.07$, wet: $p < 0.001$).

small changes in water level—both positive and negative—led to a decrease in CH_4 emissions, which meant more CH_4 was released when SRS-2 was under stable water table conditions (Figure 5e).

Lastly, the 10-day water level change had a significant impact on CH_4 fluxes during the wet season in both sites, but showed dissimilar patterns (Figure 5c, f). During the wet season in TS/Ph-1, rising water levels led to a decrease in CH_4 release and falling water levels within 0.2 m did not have a significant effect on CH_4 emission. However, when water level decreased more than 0.2 m in 10 days during the wet season in TS/Ph-1, CH_4 fluxes increased as water level decreased (Figure 5c). In SRS-2, water level change in 10 days had a strong impact on CH_4 emissions in the wet season; falling water levels led to less CH_4 release, whereas rising water level had no impact on CH_4 fluxes (Figure 5f).

In addition, although a strong relationship between higher daily or 10-day water level change and CH_4 fluxes could be observed in both sites (Figure 5b, c, e, f), few large changes were observed and thus confidence intervals were large. Therefore, the impact of large changes in water level on CH_4 fluxes in both sites over small and intermediate temporal scales remains uncertain (Figure 5a, c, d, f).

Discussion

Seasonal and Diurnal Patterns of CH_4

Similar to the findings of Dai and others (2019), Li and others (2019), and Ueyama and others (2020), both the short and long hydroperiod sites presented a pattern with higher daily CH_4 emissions during the wet seasons and lower CH_4 release during the dry seasons (Figure 2). Higher CH_4 during the summer could be due to greater methanogenesis with higher temperatures. Despite this seasonal pattern, we did not find any strong univariate correlations between daily CH_4 and any of our predictors (Figure 1). Furthermore, no obvious diurnal patterns were observed at either site (Figure S2). Although some past studies have shown distinctive peaks in CH_4 fluxes during specific time periods (Dai and others 2019; Ueyama and others 2020), other studies have not found clear diurnal patterns of CH_4 emissions throughout the year (Li and others 2018), or during specific time periods, such as the ripening stage for rice (Ge and others 2018). The combination of water management, precipitation and natural water flow in the Everglades (Beck and others 2005; Kottek and others 2006; Figure 1b) may lead to less distinctive diurnal CH_4 patterns. In addition, the tropical climate has limited temperature variation during the day in comparison to other regions. Thus, CH_4 is less likely to be impacted by micrometeorological variables like Ta on a daily scale. Lastly, the CH_4 EC data used in this research were processed without using the Eddypro diagnostic flags, which filter out high frequency fluxes that are important in ecosystems with standing water. Therefore, more variation could be present in comparison to previous studies that used these diagnostics for filtering, and this may have contributed to less clear diurnal trends compared to those seen in other studies.

Driving Factors of CH_4 by Site

Several previous studies have identified primary productivity, Ta, and water level as significant drivers of CH_4 emissions in wetlands (Silvey and others 2019; Mitsch and others 2010; Yvon-Durocher and others 2014). In agreement with these studies, both temperature and water level were determined to be strong seasonal drivers of TS/Ph-1 and SRS-2. At both sites, Ta was positively associated with CH_4 fluxes, with higher temperatures leading to more CH_4 release (Figure 3; Table 3). This relationship could be caused by faster CH_4 production as methanogens become more metabolically active with temperature increase (Simpson and others 1995; Yvon-Durocher and others 2014). A negative association was present between CH_4 and Ta in TS/Ph-1 during the wet season when Ta was above about 27 °C, suggesting that there could also be an optimal temperature for CH_4 release.

Water level was also identified to be an important predictor in both sites; however, the association between water level and CH_4 was much stronger in SRS-2, and the effects were opposite by site, especially during the wet season. Higher water level led to more CH_4 release in the short-hydroperiod site, TS/Ph-1, during the dry season, when water level can fall below the surface (Figure 1b). Higher water level in this site likely promoted the anaerobic conditions for CH_4 formation, and therefore, increased CH_4 emissions (Dai and others 2019; Hemes and others 2018). CH_4 oxidation, however, also happens under anaerobic conditions and therefore, CH_4 could be oxidized before reaching the atmosphere, especially in deeper water (Bloom 2010). In addition, since plant aerenchymas are an important pathway for CH_4 emissions (Jeffrey and others 2019), when water level is higher than mean plant canopy height ($\sim$ 1.02 m) in SRS-2, plants are fully submerged and thus limited gaseous transport leads to reduced CH_4 release. Thus, due to high water levels in the long hydroperiod site, SRS-2 (Figure 1b), CH_4 emission could be significantly reduced by the deep-water column, leading to a negative association between water level and CH_4 fluxes (Figure 4e). Lastly, Knox and others (2016) found that some CH_4 drivers were stronger at different water depths. During the dry season in both TS/Ph-1 and SRS-2, small CH_4 peaks were observed at different water levels. Higher water level was observed to drive more CH_4 release at the short hydroperiod site, but not at the long hydroperiod site. On the other hand, the predictive power of the short hydroperiod site model was less than that of the long hydroperiod, indicating that additional factors may be contributing to CH_4 emissions.

Although plant productivity has been reported to have a strong association with CH_4 emissions (Whiting and Chanton 1993), GEE was removed from the TS/Ph-1 model due to its insignificance and was only found to be a significant driver of CH_4 fluxes during the dry season for SRS-2 (Figure 3f; Table 3). Plant productivity is considered an important determinant of CH_4 because recent photosynthate can translocate from plant roots in the rhizosphere to the soil (Van Veen and others 1989), and thus, contribute to methanogenesis (Dorodnikov and others 2011). Based on previous research on CO_2 exchange in TS/Ph-1 and SRS-2, both sites were not strong carbon sinks and at times, were carbon sources (Schedlbauer and others 2010; Jimenez and others 2012). Therefore, due to low productivity the contribution of plant photosynthates to CH_4 emissions is likely negligible. However, during specific times during the dry season in the long hydroperiod site, greater CH_4 release was observed with higher photosynthesis (Figure 3e), which could contribute to a greater range of productivity values available for estimating models over the course of the study (Figure 1d).

Although daily change in mean atmospheric pressure or daily change in maximum pressure, is linked to changing weather conditions in the Everglades, pressure change was not found to be a significant predictor of CH_4 fluxes in either site. Although previous research suggested that free-phase CH_4 release in wetlands could be triggered by a drop in pressure there has been little research to validate this idea (Tokida and others 2007). Pressure change is mainly related to ebullition of CH_4 in wetlands, which is difficult to differentiate from diffusive fluxes using the EC method since ebulition is often filtered out, unlike when using floating chamber methods which can be set up to specifically separate and quantify ebullition (Staudhammer and others 2022; Deemer and Holgerson 2021). Although our findings of significance between biophysical variables and CH_4 were in agreement with previous research, our results present more complex functional relationships with CH_4 fluxes, which show predicting future CH_4 release in tropical and subtropical wetlands will be challenging even with known drivers.

Water Level Dynamics

Examination of water level changes in the Everglades could aid our ability to predict CH_4 fluxes as water level rises and falls (Kottek and others 2006; WRDA 2000). Precipitation's impact on water level is reflected by wet and dry seasons, and water distribution by the water management is apparent, for example, observed at the end of 2020 (Figure 1b). In addition, water levels in tropical and subtropical wetlands may fluctuate further due to climate change-related increases in intense rainfall events, especially in the wet season.

Future climate change may subject the Everglades to seasonal alterations in precipitation, leading to changes in water levels and inundation periods (Stanton and Ackerman 2007; IPCC 2013). Wet season precipitation is projected to decrease by 5–10%, and annual precipitation is estimated to be altered by − 2 to + 14%, with greater dry periods between heavier rain events (Christensen and others 2007; IPCC 2013). Therefore, we used a 30-day moving average to characterize prognostic, longer-term wetting, and drying trends. Although the model showed that SRS-2 could be a CH_4 sink when there was longer-term drying (Figure 5d), addtional CH_4 observations when water levels are low are needed to enhance our understanding of CH_4 sequstration. This possible sink could be due to more CH_4 oxidation when soil is saturated but there was no water above soil to ensure the anaerobic conditions for CH_4 production (Whalen and Reeburgh 1996).

Aside from greater water level change on a 30-day scale, daily water level fluctuations were also examined. Past studies have explored concurrent water level's impact on CH_4 emission under different depths (for example, Knox and others 2015); however, the impact of small-scale water level fluctuation on CH_4 release with the EC method is still uncertain, since the EC footprint covers a larger area which incorporates greater topography and variation in water table depths versus estimates from static chamber measurements. Small and intermediate scale water level change allowed us to explore timing of water level management since various scales of water fluctuations during different seasons and hydroperiods could lead to changes in CH_4 emissions. In contrast to the results from the biophysical model, the water dynamics model provides evidence that water level fluctuation could have significant impacts on CH_4 fluxes (Figure 5b, e). Moreover, compared to TS/Ph-1, the SRS-2 site is more stable. Since water level does not drop below the soil surface in SRS-2, a decrease in the number and magnitude of rainfall events and/or sudden drops in water level may have less impact on CH_4 (Ho and others 2018).

Lastly, water level change over 10-days provides an intermediate measure, between daily water fluctuation and 30-day water level trend. This measure could capture potential lagged effects of water level change on CH_4 emission (Tangen and Bansal 2019). In this research, direction of water level change was only significant during the wet seasons in both sites (Figure 5c, f). Previous research that explored the impact of changing water levels suggests that there is more CH_4 emission when water level decreases (Hondula and others 2021), as seen in TS/Ph-1 during the wet season. In contrast, a drop of water level in SRS-2 during the wet season led to lower CH_4 emission. These site-specific models, however, had differences in explanatory power. As with the biophysical model, the short hydroperiod model had lower explanatory power, suggesting that additional factors not included the model could be driving CH_4, indicating the need for additional studies that specifically investigate this uncertainty. Nonetheless, the timing of water distribution to the Everglades and future precipitation shift due to climate change could cause changes in CH_4 fluxes both seasonally and by site based on topography and inundation periods.

Uncertainties and Limitations

The greatest uncertainty in this research stems from the large data gaps due to instrument malfunction and Hurricane Irma (Figure 2). Different from previous studies with similar aims which focused on examining drivers for CH_4 fluxes in wetlands, this research used non-gap filled CH_4 data (Yu and others 2013; Li and others 2018, Dai and others 2019). The gaps in 2016 in TS/Ph-1 led to insufficient data for analysis, which was exacerbated by the different water level patterns present, that is, with less difference between the short and long hydroperiod site. Without these data, we were unable to compare the two sites when they had similar inundation conditions throughout the year (Figure 1b).

For this research, our filtering protocols resulted in retaining more spikes of CH_4 emissions compared to previous research with CH_4 flux data processed with Eddypro diagnostics flag on. This approach may have led to a higher amount of noise in our data and a lack of ability to pick up significant trends. We also acknowledge that summary variables computed at 30- and 10- day time scales are arbitrary; however, they provide a coarse measure of how prognostic, longer-term wetting, and drying trends, as well as the water level change in the Everglades, could impact CH_4 emissions. The results provide insights into the impact of future water management in natural wetlands, such as how distributing water in different seasons could impact CH_4 fluxes.

Conclusions

Our research provided new insight into the drivers of CH_4 emissions in subtropical/tropical natural wetlands using continuous data from EC observations. It also explored a new direction of understanding how different temporal scales of water level change impact CH_4 fluxes. Using 5 years of EC data from 2016 to 2020, we examined the patterns of diurnal and seasonal CH_4 fluxes, as well as the drivers of CH_4 in short and long hydroperiod sites in the Everglades. Although there were no distinctive diurnal patterns of CH_4 emissions in both the short and long hydroperiod sites, a seasonal pattern with higher CH_4 release during the wet season and lower CH_4 emissions during the dry season was observed, especially in the long hydroperiod site. Ta and water level were significant drivers of CH_4 in both seasons and both sites. Although previous studies have suggested that plant productivity was considered as one of the most important predictors for CH_4, our results showed that GEE was significantly associated with CH_4 only during the dry season in the long hydroperiod site. In addition, pressure change was not a significant driver for CH_4 in either site, which may be due to the fact that CH_4 fluxes through ebullition might not be captured by the EC method. Importantly, prolonged drying and wetting conditions, daily water level change, and 10-day water level change all had impacts on CH_4 release which varied between seasons and sites. These results indicate that water dynamics interact strongly with site characteristics in determining CH_4 emissions. Therefore, CH_4 release pattern, and its drivers, such as Ta and water level, will likely be altered by future climate change. Moreover, as the implementation of CERP moves forward, the amount and timing of water distribution are predicted to change and could potentially lead to different seasonal hydrological patterns. The knowledge gained in this study will help to better estimate CH_4 budgets in the future and allow better predictions of the CH_4 source or sink capacity for the Everglades.

ACKNOWLEDGEMENTS

All research was performed under permits issued by Everglades National Park (EVER-2009-SCI- 0070 and EVER-2013-SCI-0058). The authors would like to acknowledge the excellent support provided by the Florida Coastal Everglades Long Term Ecological Research Program (FCE-LTER) and the Southeast Environmental Research Center in the Institute of Water and Environment at Florida International University. This manuscript is partly based upon work supported by the National Science Foundation (NSF) through the FCE-LTER program under Grant DEB-1237517. This research is also based in part on support from the Department of Energy's (DOE) National Institute for Climate Change Research (NICCR) through grant 07-SC-NICCR-1059 and the National Science Foundation Division of Atmospheric and Geospace Sciences Atmospheric Chemistry Program awards 1561139, 1233006, 1801310 and 1807533. This research was also supported by the ForEverglades Foundation. Any opinions, findings, and conclusions or recommendations expressed in this material are those of the authors and do not necessarily reflect the views of FCE-LTER, NSF, or DOE.

DATA AVAILABILITY

Eddy covariance data and corresponding micrometeorological data are archived through the Ameriflux repository (https://ameriflux.lbl.gov/sites/site info/US-Elm and https://ameriflux.lbl.gov/sites/siteinfo/US-Esm).

REFERENCES

Alberto MCR, Wassmann R, Buresh RJ, Quilty JR, Correa TQ Jr, Sandro JM, Centeno CAR. 2014. Measuring methane flux from irrigated rice fields by eddy covariance method using open-path gas analyzer. Field Crops Res 160:12–21.

Armentano TV, Sah JP, Ross MS, Jones DT, Cooley HC, Smith CS. 2006. Rapid responses of vegetation to hydrological changes in Taylor Slough, Everglades National Park, Florida, USA. Hydrobiologia 569(1):293–309.

Bansal S, Tangen B, Finocchiaro R. 2016. Temperature and hydrology affect methane emissions from prairie pothole Wetlands. Wetlands 36:S371–S381. https://doi.org/10.1007/s13157-016-0826-8.

Beck C, Grieser J, Kottek M, Rubel F, Rudolf B. 2005. Characterizing global climate change by means of köppen climate classification. Klimastatusbericht 51:139–149.

Bloom AA, Palmer PI, Fraser A, Reay DS, Frankenberg C. 2010. Large-scale controls of methanogenesis inferred from methane and gravity spaceborne data. Science 327(5963):322–325.

Burba GG, Verma SB, Kim J. 1999. Surface energy fluxes of phragmites australis in a prairie wetland. Agric For Meteorol 94(1):31–51.

Chang KY, Riley WJ, Knox SH, et al. 2021. Substantial hysteresis in emergent temperature sensitivity of global wetland CH_4 emissions. Nat Commun 12:2266. https://doi.org/10.1038/s41467-021-22452-1.

Christensen JH, Hewitson B, Busuioc A, Chen A, Gao X, Held I, Jones R, Kolli RK, Kwon WT, Laprise R, Magana Rueda V. 2007. Contribution of working group I to the fourth assessment report of the intergovernmental panel on climate change. Clim Change 6:848–940.

Ciais P, Sabine C, Bala G, Bopp L, Brovkin V, Canadell J, Heimann M. 2013. Carbon and other biogeochemical cycles. Climate change 2013: the physical science basis. contribution of working group I to the fifth assessment report of the intergovernmental panel on climate change. Comput Geom 18:95–123.

Clark KL, Gholz HL, Moncrieff JB, Cropley F, Loescher HW. 1999. Environmental controls over net exchanges of carbon dioxide from contrasting florida ecosystems. Ecol Appl 9(3):936–948.

Dai S, Ju W, Zhang Y, He Q, Song L, Li J. 2019. Variations and drivers of methane fluxes from a rice-wheat rotation agroecosystem in eastern china at seasonal and diurnal scales. Sci Total Environ 690:973–990. https://doi.org/10.1016/j.scitotenv.2019.07.012.

Davis S, Ogden JC. 1994. Everglades: the ecosystem and its restoration. CRC Press.

Deemer BR, Holgerson MA. 2021. Drivers of methane flux differ between lakes and reservoirs, complicating global upscaling efforts. J Geophys Res Biogeosci 126(4):e2019JG005600.

Delwiche KB, Knox SH, Malhotra A, Fluet-Chouinard E, McNicol G, Feron S, Jackson RB (2021). FLUXNET-CH4: A global, multi-ecosystem dataset and analysis of methane seasonality from freshwater wetlands

Detto M, Verfaillie J, Anderson F, Xu L, Baldocchi D. 2011. Comparing laser-based open-and closed-path gas analyzers to measure methane fluxes using the eddy covariance method. Agricul For Meteorol 151(10):1312–1324.

Dlugokencky EJ, Bruhwiler L, White JWC, Emmons LK, Novelli PC, Montzka SA, Masarie KA, Lang PM, Crotwell AM, Miller JB, Gatti LV. 2009. Observational constraints on recent increases in the atmospheric CH_4 burden. Geophys Res Lett. https://doi.org/10.1029/2009GL039780.

Dorodnikov M, Knorr K, Kuzyakov Y, Wilmking M. 2011. Plant-mediated CH 4 transport and contribution of photosynthates to methanogenesis at a boreal mire: A 14 C pulse-labeling study. Biogeosciences 8(8):2365–2375.

Duever MJ, Carlson JE, Riopelle LA, Gunderson LH, Duever LC. Ecosystem analyses at Corkscrew Swamp. Third Annual Report on Cypress Wetlands, Florida University, Center for Wetlands, Gainesville p 707-737, 1976. 9 fig, 5 tab, 4 ref. 1976.

Duever MJ, Meeder JF, Meeder LC, McCollom JM. The climate of south Florida and its role in shaping the Everglades ecosystem. Everglades: The ecosystem and its restoration. 1994:225-248.

Foken T, Leclerc MY. 2004. Methods and limitations in validation of footprint models. Agric For Meteorol 127(3–4):223–234.

Foken T, Wichura B. 1996. Tools for quality assessment of surface-based flux measurements. Agric For Meteorol 78(1–2):83–105.

Fratini G, Mauder M. 2014. Towards a consistent eddy-covariance processing: an intercomparison of EddyPro and TK3. Atmos Meas Tech 7(7):2273–2281.

Ge HX, Zhang HS, Zhang H, Cai XH, Song Y, Kang L. 2018. The characteristics of methane flux from an irrigated rice farm in East China measured using the eddy covariance method. Agric For Meteor 249:228–238. https://doi.org/10.1016/j.agrformet.2017.11.010.

Goulden ML, Munger JW, Fan S, Daube BC, Wofsy SC. 1996. Measurements of carbon sequestration by long-term eddy covariance: Methods and a critical evaluation of accuracy. Global Change Biology 2(3):169–182.

Gottlieb AD, Richards JH, Gaiser EE. 2006. Comparative study of periphyton community structure in long and short hydroperiod Everglades marshes. Hydrobiologia 569:195–207.

Haman DZ, Svendsen M. 2006. Managing the Florida Everglades: Changing values, changing policies. Irrig Drain Syst 20(2–3):283–302. https://doi.org/10.1007/s10795-006-9008-9

Hastie T, Tibshirani R. 1986. Generalized additive models. Stat Sci 1(3):297–318.

Helbig M, Quinton WL, Sonnentag O. 2017. Warmer spring conditions increase annual methane emissions from a boreal peat landscape with sporadic permafrost. Environ Res Lett 12(11):115009.

Hemes KS, Chamberlain SD, Eichelmann E, Knox SH, Baldocchi DD. 2018. A biogeochemical compromise: the high methane cost of sequestering carbon in restored wetlands. Geophys Res Lett 45(12):6081–6091. https://doi.org/10.1029/2018GL077747.

Ho DT, Engel VC, Ferrón S, Hickman B, Choi J, Harvey JW. 2018. On factors influencing air-water gas exchange in emergent wetlands. J Geophys Res Biogeosci 123(1):178–192.

Hondula KL, Jones CN, Palmer MA. 2021. Effects of seasonal inundation on methane fluxes from forested freshwater wetlands. Environ Res Lett 16(8):084016.

Jeffrey LC, Maher DT, Johnston SG, Kelaher BP, Steven A, Tait DR. 2019. Wetland methane emissions dominated by plant-mediated fluxes: Contrasting emissions pathways and seasons within a shallow freshwater subtropical wetland. Limnol Oceanography 64(5):1895–1912.

Jimenez KL, Starr G, Staudhammer CL, Schedlbauer JL, Loescher HW, Malone SL, Oberbauer SF. Carbon dioxide exchange rates from short-and long-hydroperiod Everglades freshwater marsh. Journal of Geophysical Research: Biogeosciences. 2012;117(G4).

Kim J, Verma SB, Billesbach DP. 1999. Seasonal variation in methane emission from a temperate phragmites-dominated marsh: effect of growth stage and plant-mediated transport. Global Change Biol 5(4):433–440.

Kirschke S, Bousquet P, Ciais P, Saunois M, Canadell JG, Dlugokencky EJ, Bruhwiler L. 2013. Three decades of global methane sources and sinks. Nat Geosci 6(10):813–823.

Kljun N, Rotach MW, Schmid HP. 2002. A three-dimensional backward lagrangian footprint model for a wide range of boundary-layer stratifications. Boundary-Layer Meteorol 103(2):205–226.

Kljun N, Calanca P, Rotach MW, Schmid HP. 2004. A simple parameterisation for flux footprint predictions. Boundary-Layer Meteorol 112(3):503–523.

Knox SH, Sturtevant C, Matthes JH, Koteen L, Verfaillie J, Baldocchi D. 2015. Agricultural peatland restoration: effects of land-use change on greenhouse gas (CO2 and CH4) fluxes in the Sacramento-San joaquin delta. Global Change Biol 21(2):750–765.

Kottek M, Grieser J, Beck C, Rudolf B, Rubel F. 2006. World map of the köppen-geiger climate classification updated. Meteorologische Zeitschrift 15(3):259–263.

Lan X, Nisbet EG, Dlugokencky EJ, Michel SE. 2021. What do we know about the global methane budget? Results from four decades of atmospheric CH4 observations and the way forward. Phil Trans R Soc A 379:20200440. https://doi.org/10.1098/rsta.2020.0440

Li H, Dai S, Ouyang Z, Xie X, Guo H, Gu C, Zhao B. 2018. Multi-scale temporal variation of methane flux and its controls in a subtropical tidal salt marsh in eastern china. Biogeochemistry 137(1):163–179.

Li H, Guo H, Helbig M, Dai S, Zhang M, Zhao M, Zhao B. 2019. Does direct-seeded rice decrease ecosystem-scale methane emissions? A case study from a rice paddy in southeast china. Agric For Meteorol 272:118–127.

Liu L, Wang D, Chen S, Yu Z, Xu Y, Ge Z, Chen Z. 2019. Methane emissions from estuarine coastal wetlands: implications for global change effect. Soil Biol Biochem. https://doi.org/10.2136/sssaj2018.12.0472.

Ma L, Liu B, Cui Y, Shi Y. 2021. Variations and drivers of methane fluxes from double-cropping paddy fields in Southern China at Diurnal, seasonal and inter-seasonal timescales. Water 13(16):2171. https://doi.org/10.3390/w13162171

Malone SL, Staudhammer CL, Loescher HW, Olivas P, Oberbauer SF, Ryan MG, Starr G. 2014. Seasonal patterns in energy partitioning of two freshwater marsh ecosystems in the Florida everglades. J Geophys Res Biogeosci 119(8):1487–1505.

McDermitt D, Burba G, Xu L, Anderson T, Komissarov A, Riensche B, Oechel W. 2011. A new low-power, open-path instrument for measuring methane flux by eddy covariance. Applied Phys B 102(2):391–405.

Misra V, Bhardwaj A, Mishra A. 2018. Characterizing the rainy season of peninsular Florida. Clim Dynamics 51(5):2157–2167.

Mitsch WJ, Nahlik A, Wolski P, Bernal B, Zhang L, Ramberg L. 2010. Tropical wetlands: seasonal hydrologic pulsing, carbon sequestration, and methane emissions. Wetlands Ecol Manage 18(5):573–586.

Morin TH, Bohrer G, Frasson R. 2014. Environmental drivers of methane fluxes from an urban temperate wetland park. J Geophys Res Biogeosci 119(11):2188–2208.

Noska R, Misra V. 2016. Characterizing the onset and demise of the indian summer monsoon. Geophys Res Lett 43(9):4547–4554.

Obeysekera J, Browder J, Hornung L, Harwell MA. 1999. The natural south Florida system I: climate, geology, and hydrology. Urban Ecosyst 3(3):223–244.

Peltola O, Mammarella I, Haapanala S, Burba G, Vesala T. 2013. Field intercomparison of four methane gas analyzers suitable for eddy covariance flux measurements. Biogeosciences 10(6):3749–3765.

Peltola O, Hensen A, Helfter C, Belelli Marchesini L, Bosveld FC, Van Den Bulk W, Laurila T. 2014. Evaluating the performance of commonly used gas analysers for methane eddy covariance flux measurements: the InGOS inter-comparison field experiment. Biogeosciences 11(12):3163–3186.

Rosentreter JA, Borges AV, Deemer BR, Holgerson MA, Liu S, Song C, Eyre BD. 2021. Half of global methane emissions come from highly variable aquatic ecosystem sources. Nat Geosci 14(4):225–230.

Saunois M, Stavert AR, Poulter B, Bousquet P, Canadell JG, Jackson RB, Patra PK. 2020. The global methane budget 2000–2017. Earth Syst Sci Data 12(3):1561–1623.

Schedlbauer JL, Oberbauer SF, Starr G, Jimenez KL. 2010. Seasonal differences in the CO_2 exchange of a short-hydroperiod Florida everglades marsh. Agric For Meteorol 150(7–8):994–1006.

SFWMD. (1999). South Florida Water Management District. Retrieved from https://www.sfwmd.gov/

Silvey C, Jarecke KM, Hopfensperger K, Loecke TD, Burgin AJ. 2019. Plant species and hydrology as controls on constructed wetland methane fluxes. Soil Sci Soc Am J 83(3):848–855.

Simpson IJ, Thurtell GW, Kidd GE, Lin M, Demetriades-Shah TH, Flitcroft ID, Neue HU. 1995. Tunable diode laser measurements of methane fluxes from an irrigated rice paddy field in the philippines. J Geophys Res Atmosp 100(D4):7283–7290.

Stanton EA, Ackerman F. Florida and climate change: the costs of inaction. Florida and climate change: the costs of inaction. 2007

Staudhammer CL, Malone SL, Zhao J, Yu Z, Starr G, Oberbauer SF. 2022. Methane emissions from subtropical wetlands: an evaluation of the role of data filtering on annual methane budgets. Agric For Meteorol 321:108972.

Tangen BA, Bansal S. 2019. Hydrologic lag effects on wetland greenhouse gas fluxes. Atmosphere 10(5):269.

Tokida T, Miyazaki T, Mizoguchi M, Nagata O, Takakai F, Kagemoto A, Hatano R. 2007. Falling atmospheric pressure as a trigger for methane ebullition from peatland. Glob Biogeochem Cycles 21:GB2003. https://doi.org/10.1029/2006GB002790

Ueyama M, Yazaki T, Hirano T, Futakuchi Y, Okamura M. 2020. Environmental controls on methane fluxes in a cool temperate bog. Agric For Meteorol 281:107852.

IPCC. 2021. Climate Change 2021: The Physical Science Basis. Contribution of Working Group I to the Sixth Assessment Report of the Intergovernmental Panel on Climate Change [Masson-Delmotte, V., P. Zhai, A. Pirani, S.L. Connors, C. Péan, S. Berger, N. Caud, Y. Chen, L. Goldfarb, M.I. Gomis, M. Huang, K. Leitzell, E. Lonnoy, J.B.R. Matthews, T.K. Maycock, T. Waterfield, O. Yelekçi, R. Yu, and B. Zhou (eds.)]. Cambridge University Press. In Press.

Van Veen JA, Merckx R, Van De Geijn SC. 1989. Plant-and soil-related controls of the flow of carbon from roots through the soil microbial biomass. In: Clarholm M, Bergström L, Eds. Ecology of arable land: perspectives and challenges, . Dordrecht: Springer Netherlands. pp 43–52. https://doi.org/10.1007/978-94-009-1021-8_5.

Veldkamp E, O'Brien JJ. 2000. Calibration of a frequency domain reflectometry sensor for humid tropical soils of volcanic origin. Soil Sci Soc Am J 64(5):1549–1553.

Were D, Kansiime F, Fetahi T, Hein T. 2021. Carbon dioxide and methane fluxes from various vegetation communities of a natural tropical freshwater wetland in different seasons. Environ Process 8:553–571.

Whalen SC, Reeburgh WS. 1996. Moisture and temperature sensitivity of CH_4 oxidation in boreal soils. Soil Biol Biochem 28(10–11):1271–1281.

Whiting GJ. 1993. Primary production control of methane emission from wetlands. Nature 364(6440):794–795. https://doi.org/10.1038/364794a0.

Wood SN. 2011. Fast stable restricted maximum likelihood and marginal likelihood estimation of semiparametric generalized linear models. J R Stat Soc Ser B (statistical Methodology) 73(1):3–36.

Wood SN. 2017. Generalized additive models: An introduction with R. Chapman and Hall/CRC. https://doi.org/10.1201/9781315370279.

WRDA, Water Resources Development Act 2000, Section 601 Comprehensive Everglades Restoration Plan

Yu L, Wang H, Wang G, Song W, Huang Y, Li S, He J. 2013. A comparison of methane emission measurements using eddy covariance and manual and automated chamber-based techniques in tibetan plateau alpine wetland. Environ Pollution 181:81–90.

Yu X, Song C, Sun L, Wang X, Shi F, Cui Q, Tan W. 2017. Growing season methane emissions from a permafrost peatland of northeast china: observations using open-path eddy covariance method. Atmospheric Environ 153:135–149.

Yvon-Durocher G, Allen AP, Bastviken D, Conrad R, Gudasz C, St-Pierre A, Del Giorgio PA. 2014. Methane fluxes show consistent temperature dependence across microbial to ecosystem scales. Nature 507(7493):488.

Yiming Zhang B, Naafs DA, Huang X, Song Q, Xue J, Wang R, Zhao M, Evershed RP, Pancost RD, Xie S. 2022. Variations in wetland hydrology drive rapid changes in the microbial community, carbon metabolic activity, and greenhouse gas fluxes. Geochimica et Cosmochimica Acta 317:269–285. https://doi.org/10.1016/j.gca.2021.11.014.

Zhao J, Oberbauer SF, Olivas PC, Schedlbauer JL, May JL, Moser JG, Starr G. 2018. Contrasting photosynthetic responses of two dominant macrophyte species to seasonal inundation in an everglades freshwater prairie. Wetlands 38(5):893–903.